Hooke's Law: Nonlinear Generalization and Applications

Part II Parameters of the Bending Pressure Zone of a Beam

Institute of Statistics, University of Erlangen-Nürnberg – Prof.Dr. H.Schneeberger

2021, 9th of Febr.

Keywords: Center of stress β_0, stress α_o and strain ε_o of the bending pressure zone in dependence on strength W and loading κ of concrete.

Introduction

The bending pressure zone of a pressed beam is limited by the pressed side and the neutral axis, where the strain ε is zero. If one takes, as is shown in figure 1, a prism , limited by these two boundaries, out of the beam and brings an eccentric loading to the ends, so that the strain ϵ on the section-side is zero, then one has in the prisma a copy of the disribution of the loading in the bending pressure zone ([3], p.1). See figure 1.

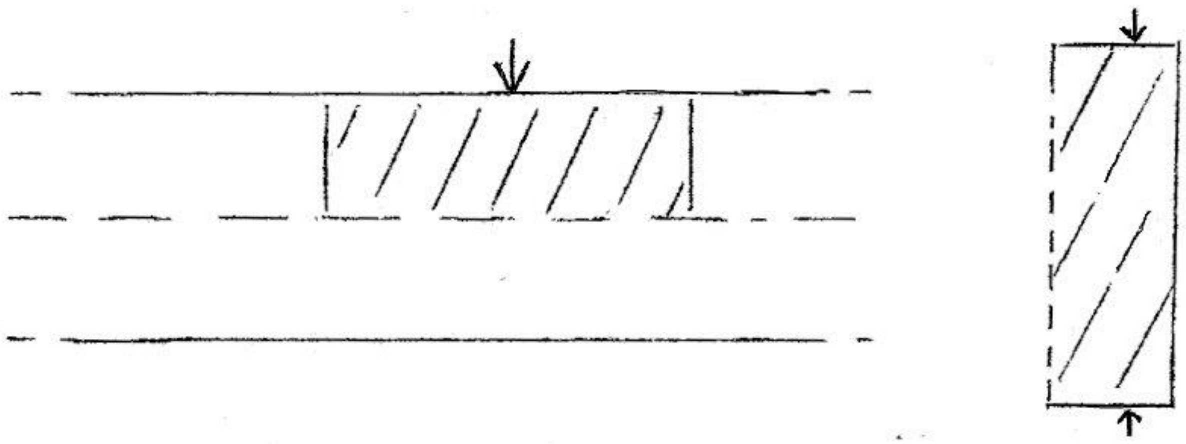

Fig. 1: Equivalence of the bending pressure zone of a beam and an eccentric pressed prism

In figure 2 a sketch of such a prisma is given (copy of [3]). For comparability I also use the symbols and measures of [3].

The problem of the extensive experiments in [3] was to find for different values of cube-strength W(kg/cm^2; side length 20 cm) and $\kappa = \bar{\sigma}/\bar{\sigma}_B$ (B for break/Bruch) the values of β_0, the measure of eccentricity of the loading of the prism in [3] and center of the distribution of the stress, and of the (relative) stress α_0^P=$\bar{\sigma}/K_b$, where K_b is the strength of the prism. These values β_0, α_0^P and ε_0(=ε_1) are found, when, by varying W and/or κ, ε_2 becomes zero.

To this at first for a fixed value of W and a fxed value of β a series experiments was done with growing stress until break.

Then the same was done with prisms (of the same W)and other values of β.

At last step 1 and 2 were done with other values of W.

In detail see [3], figures 48-88.

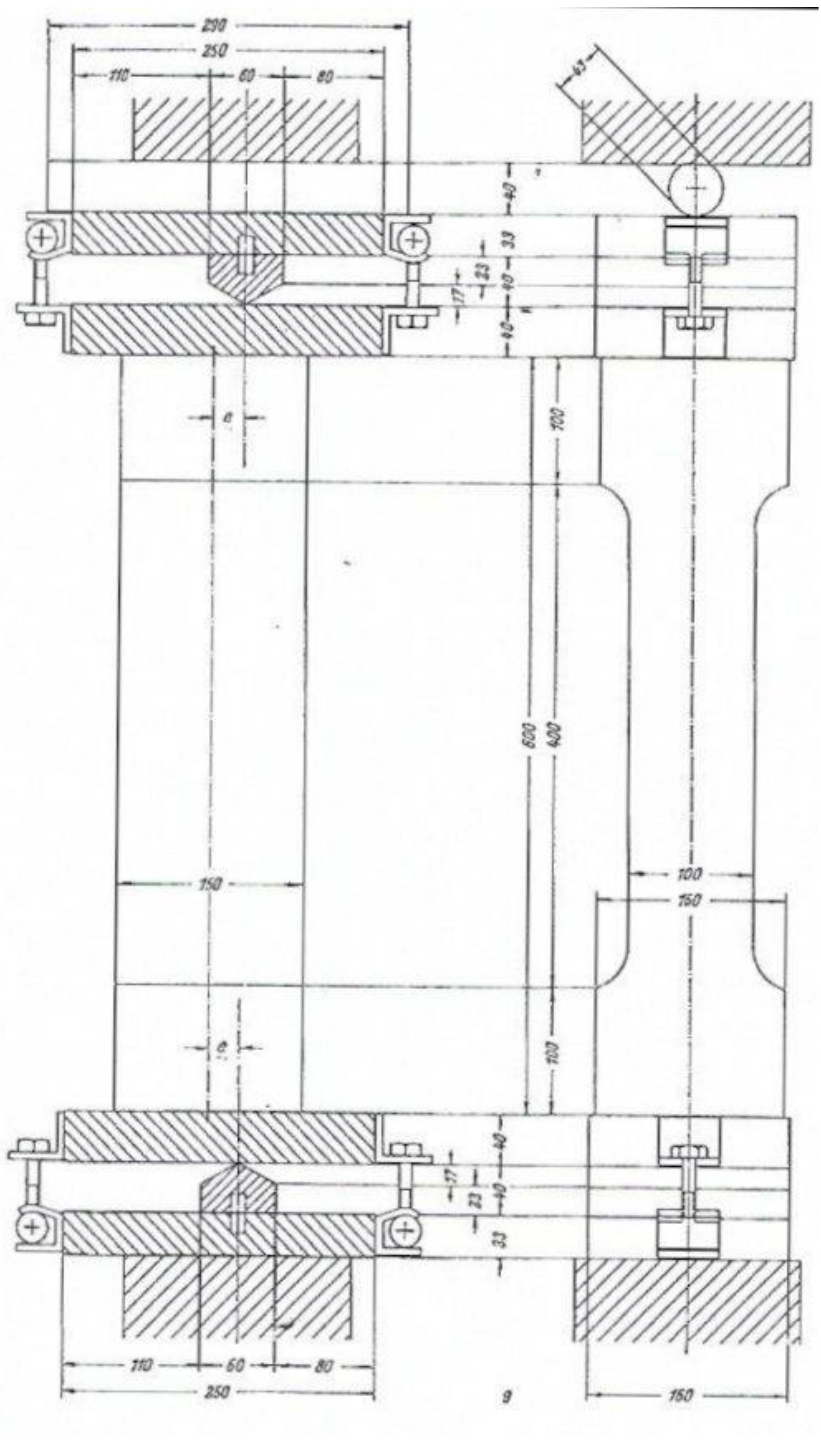

Fig. 2: Details of loading the prisms

With these data the results $\alpha^P(\beta)$, $\varepsilon_2(\beta)$ and $\varepsilon_1(\beta)$ for different values of κ *were plotted* for different values of W (see [3], figures 94-107). The essential results are the values β=$\beta_{0,}$, where ε_2=0. Then α^P=α_0^P and ε_1=ε_0. See figure 3.

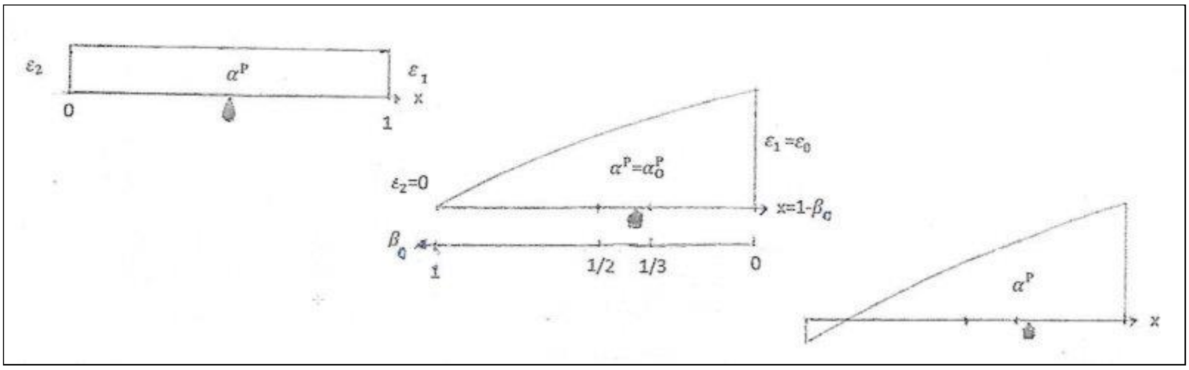

Fig. 3: Parameters strain ε, (rel) stress $\alpha_{P=}\bar{\sigma}$ /κ_b (κ_b is strength of prism) and measure of eccentricity β of loading. Eccentricity e=d(0.5-β); d=150mm

These results are given in [3], Bild 113, 112, 114 , repeated here as figures 4a, 5a, and 6a and listed in tables 1, 2, and 3. They are the experimental basis for the following analytical hypotheses.

To get truthworthy results it is of decisive importance to disregard non-truhworthy experimental data. Of this sort are are the experiments with high loading $\kappa > 0.9$. See e.g.[3]. p.24, or [2],p.74.

For this reason experimental data with κ>0.9 were ignored in the tables and in the computations.

Hypotheses

Hypothesis H1 for β_0 (and the center of loading (1-β_0))

$$\hat{\beta}_0(\mathrm{w},\kappa)=1/3+(1/2-1/3)e^{-a(W/100)}\kappa^b$$

The parameters a and b are computed with Gauss' method of least squares:

Q(a,b)=$\sum(\beta_{0i} - \hat{\beta}_{oi})^2$ → Min. (i=1,…49); the mimimum is found with the iterative nonlinear simplex-method of Nelder and Mead [1]. We get:

$$\widehat{\beta}_0=1/3+1/6\ e^{-0.3374(W/100)}\kappa^{3.757}$$

The results are given in table 1, lines 2 and especially in figure 4b : $\hat{\beta}_0\,(W)$ for fixed values of κ and in figure 4c: $\hat{\beta}_{0(}(\kappa)$ for fixed values of W. Notice the good correspondence of the hypothesis (curves) with the high number (n=49) of experimental points! Dotted curves are extrapolated.

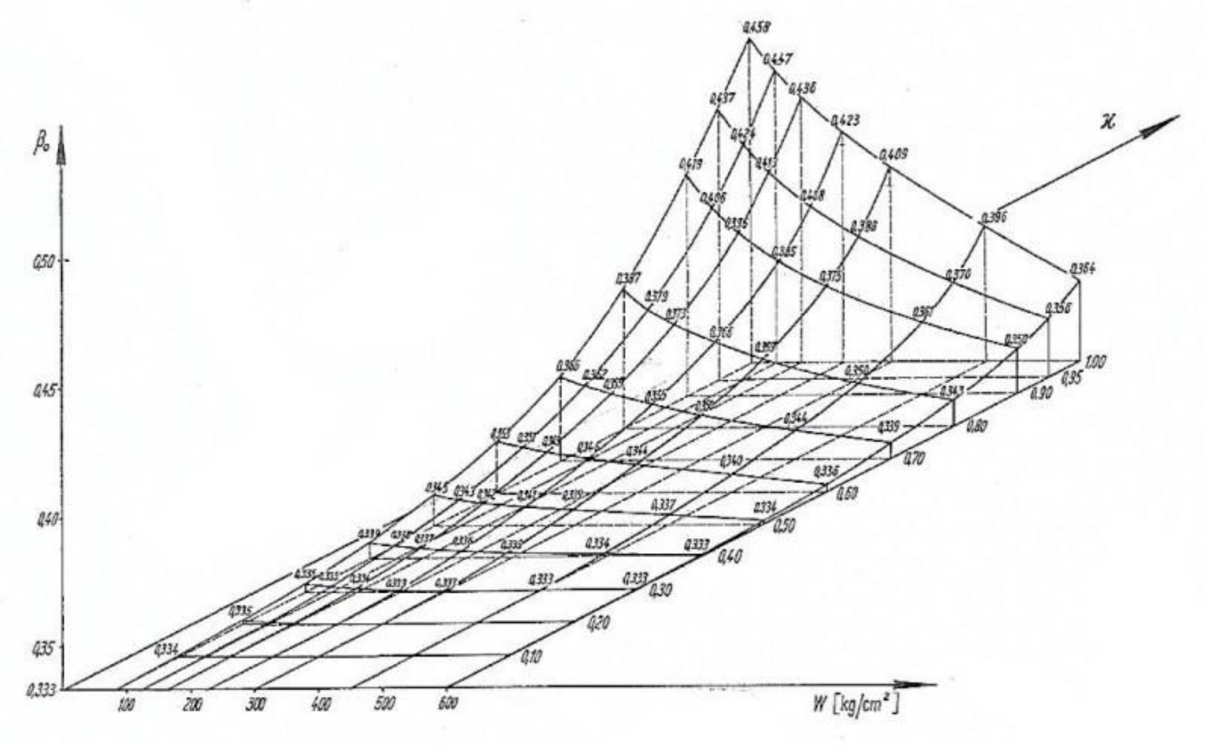

Fig. 4a: Experimental results $\beta_0(W, \kappa)$ according to [3]

Table 1: first lines: Experimental values β_0;, second lines: hypothetical values of $\widehat{\beta}_0$

W/100 kappa	.80	I.20	I.60	2.25.	3.00	4.50.	6.00
0.3	0.336	0.335	0.334	0.333	0.333	0.333	0.333
	0.335	0.335	0.334	0.334	0.334	0.334	0.333
0.4	0.339	0.338	0.337	0.336	0.335	0.334	0.333
	0.337	0.337	0.336	0.336	0.335	0.334	0.334
0.5	0.345	0.343	0.342	0.341	0.339	0.337	0.334
	0.343	0.342	0.341	0.339	0.338	0.336	0.335
0.6	0.353	0.351	0.349	0.346	0.344	0.340	0.336
	0.352	0.350	0.348	0.344	0.342	0.339	0.337
0.7	0.365	0.362	0.359	0.355	0.350	0.344	0.339
	0.367	0.362	0.359	0.354	0.349	0.343	0.339
0.8	0.387	0.379	0.373	0.366	0.359	0.350	0.343
	0.388	0.381	0.375	0.367	0.360	0.349	0.343
0.9	0.419	0.406	0.396	0.385	0.375	0.361	0.360
	0.419	0.408	0.399	0.386	0.374	0.358	0.348

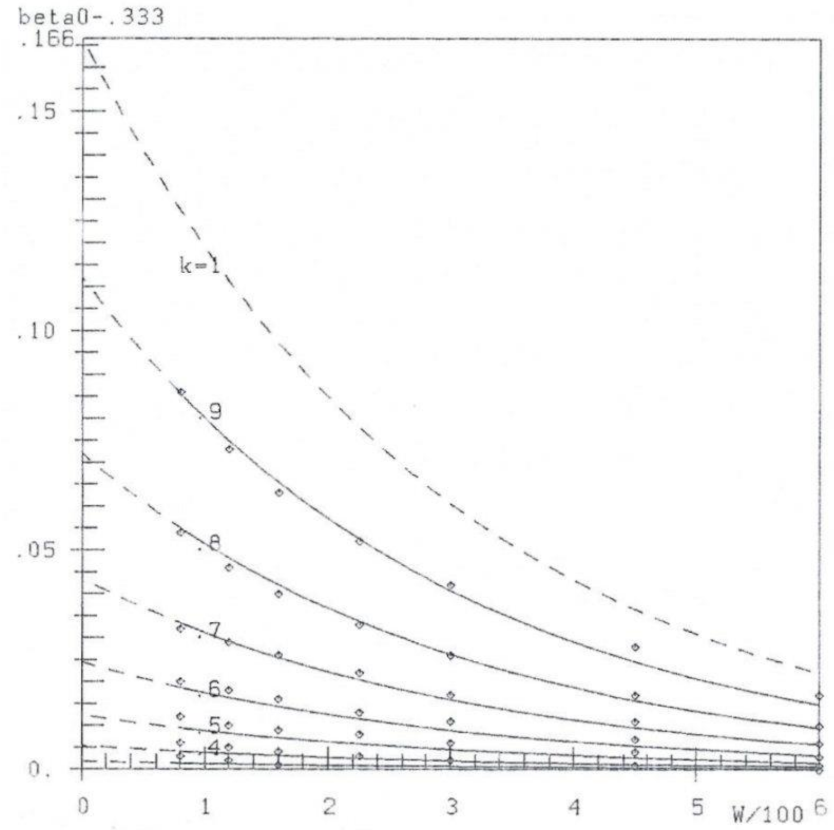

Fig. 4b: Experimental points (W/100, β_0-0.333) and hypothetical curves (W/100, $\widehat{\beta}_0$-0.333)

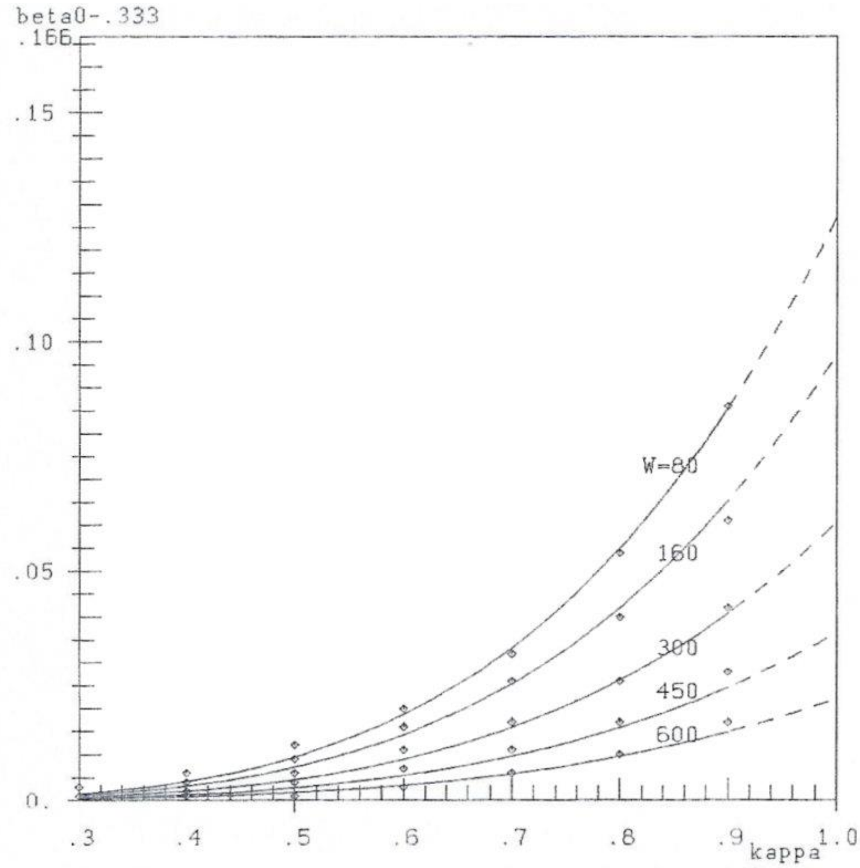

Fig. 4c: Experimental points (κ, β_0-0.333) and hypothetical curves ($\hat{\kappa}$, $\widehat{\beta}_0$-0.333)

Hypothesis H2 for the (relative) loading $\alpha_0^p=\bar{\sigma}_0/K_b$:

$$\boldsymbol{\hat{\alpha}_0^p(W,\kappa)=(2/3)\kappa+(1/3)e^{-a(W/100)}\kappa^b}$$

The analogous calculation as with hypothesis H1 , now with the 49 data of table 2 gives:

$$\hat{\alpha}_0^p=(2/3)\kappa+1/3\ e^{-0.4052(\frac{W}{100})}\kappa^{5.846}$$

The results are given in table 2, lines 2 and in figures 5b and 5c. Especially in figure 5b correspondence of data-poins and hypothetical curves is very convincing– with one exception!

For high loading ($\kappa = 0.9$) and small values of W. For this also see [3], p.24.

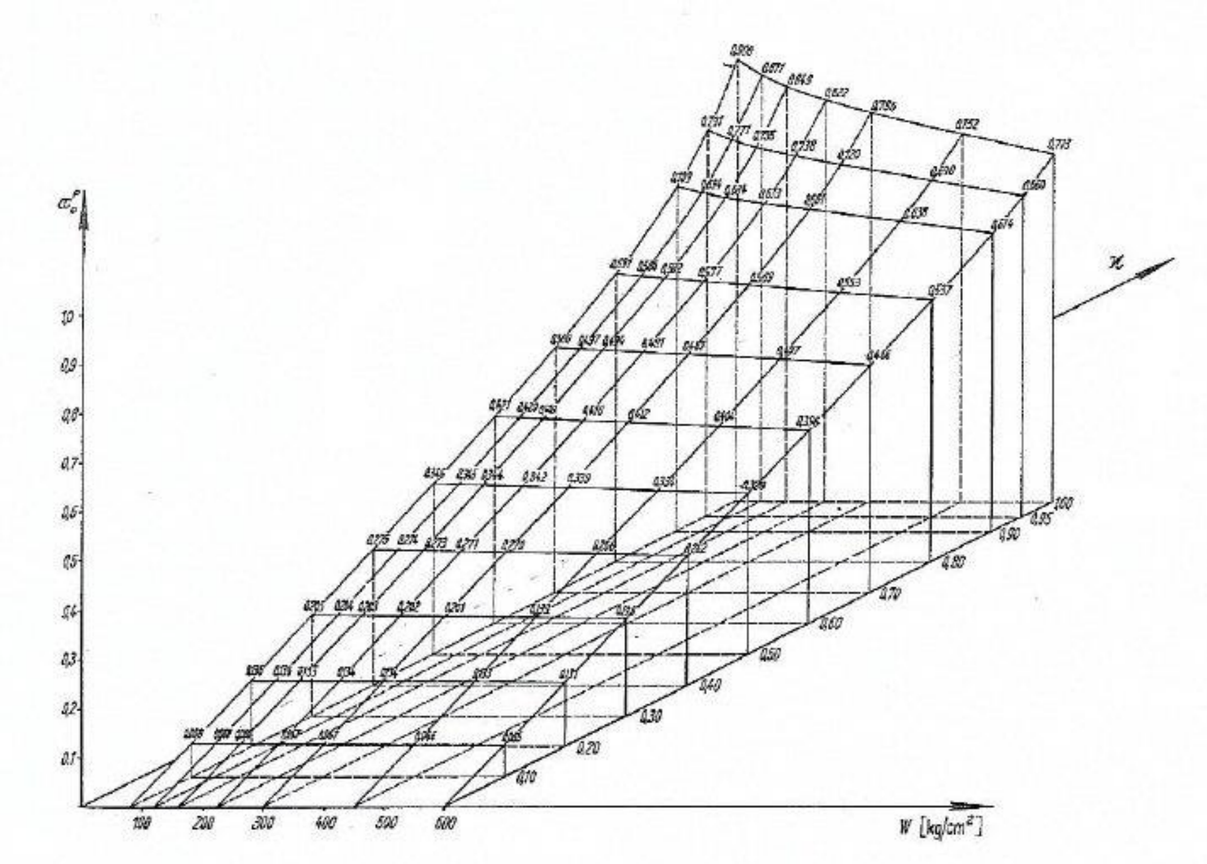

Fig. 5a: Experimental results $\boldsymbol{\alpha_0^p}$ (W, κ) according to [3]

Table 2: First lines: experimental values $\boldsymbol{\alpha}_0^P$, second lines: hypothetical values $\hat{\alpha}_0^p$

W/100 kappa	0.80	I.20	I.60	2.25.	3.00	4.50.	6.00
0.3	0.205	0.204	0.203	0.202	0.201	0.199	0.196
	0.202	0.202	0.202	0.201	0.201	0.200	0.200
0.4	0.275	0.274	0.273	0.271	0.270	0.266	0.262
	0.268	0.268	0.267	0.267	0.267	0.266	0.266
0.5	0.346	0.345	0.344	0.342	0.339	0.334	0.328
	0.338	0.337	0.336	0.336	0.335	0.334	0.333
0.6	0.421	0.420	0.418	0.416	0.412	0.404	0.396
	0.412	0.410	0.409	0.407	0.405	0.403	0.401
0.7	0.500	0.497	0.494	0.491	0.487	0.477	0.466
	0.497	0.492	0.488	0.483	0.479	0.473	0.470
0.8	0.591	0.586	0.582	0.577	0.569	0.553	0.537
	0.599	0.589	0.580	0.569	0.560	0-547	0.541
0.9	0.709	0.694	0.684	0.673	0.661	0.638	0.614
	0.730	0.710	0.694	0.672	0.653	0.629	0.616

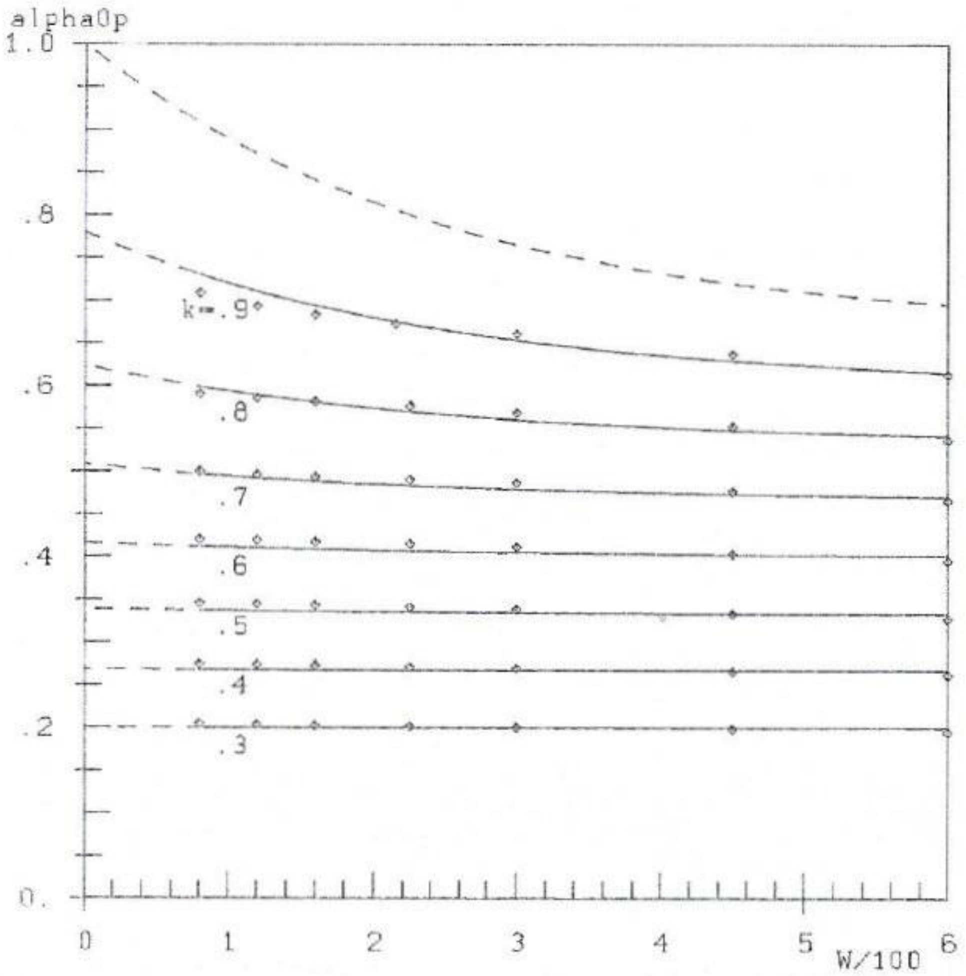

Figure 5b: experimental points (W/100, $\boldsymbol{\alpha}_0^P$) and hypothetical curves (W/100, $\hat{\alpha}_0^p$)

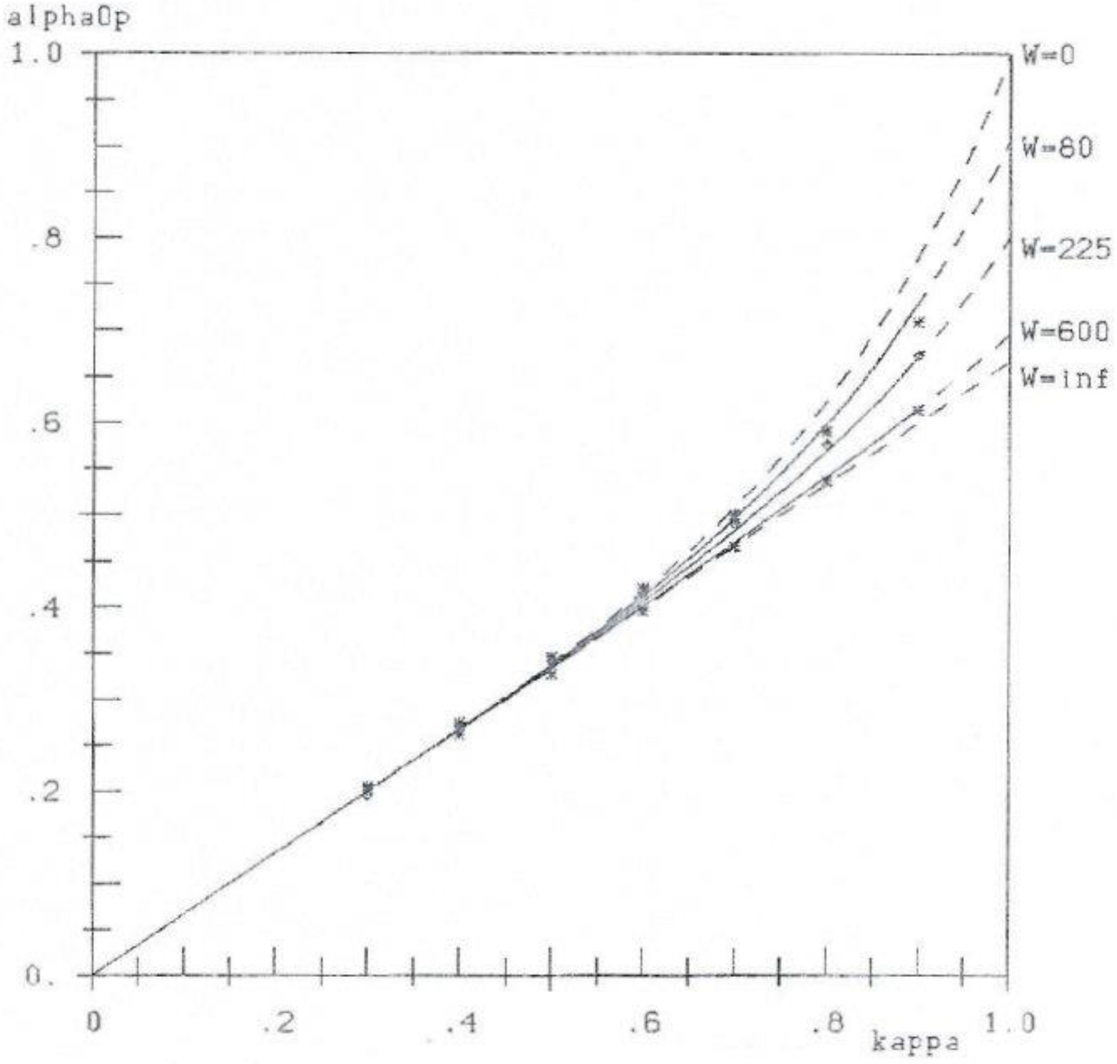

Fig. 5c: experimental points (κ, $\boldsymbol{\alpha}_{\mathbf{0}}^{\boldsymbol{P}}$) and hypothetical curves (κ, $\hat{\alpha}_0^p$)

Hypothesis H3 for the stress-strain relation with **non-centric** loading:

$$\hat{\kappa}=a\varepsilon_0 e^{-b\varepsilon_o}$$

„The stress-strain relationship for non-centric loading is the same as that for centric loading".

See [4].

The (now 63) experimental data (ε_o,κ) are given in table 3a, lines 1 and 2, the hypothetical results $\hat{\kappa}$ in line 3. The parameters a and b for 7 values of W are given in table 3b. Figure 6b shows the correspondence of data and hypothesis.

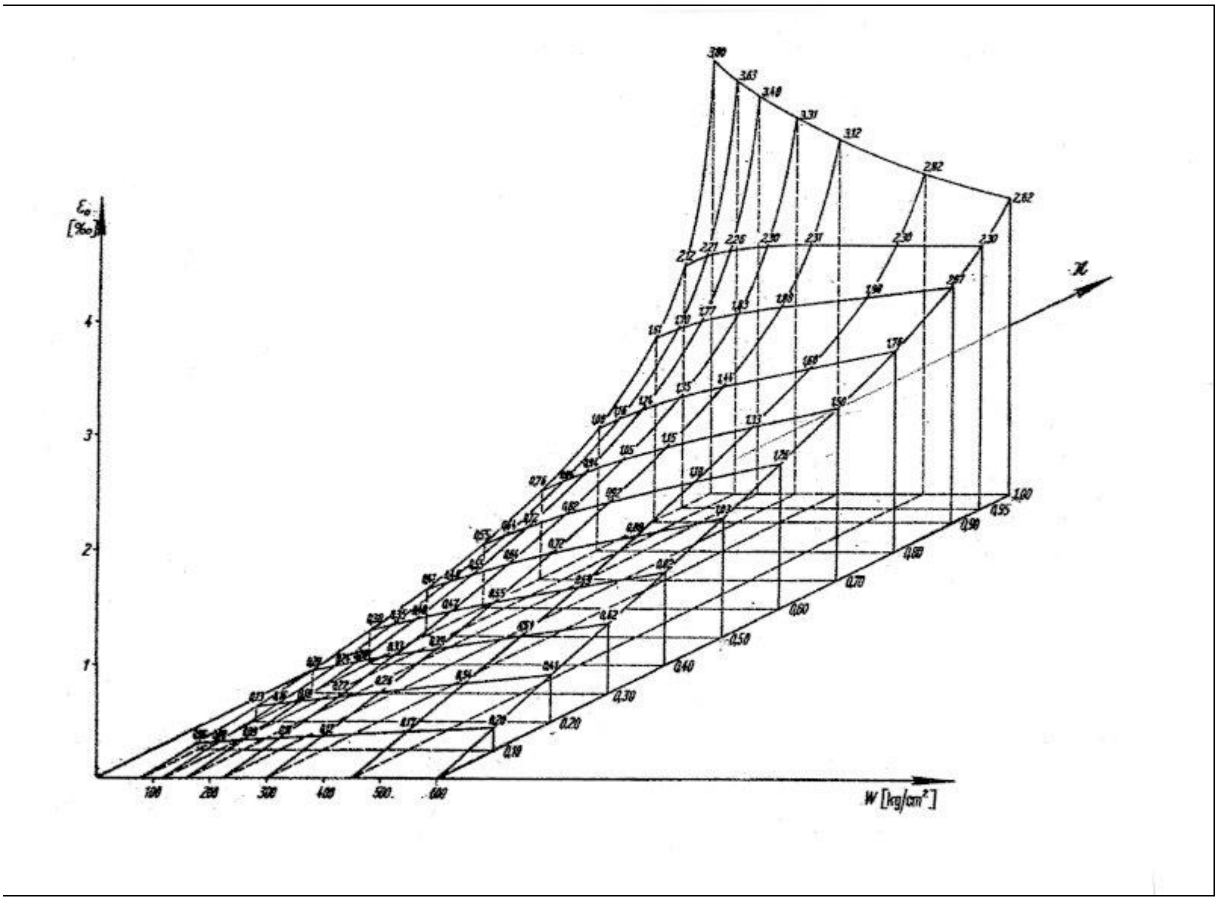

Fig. 6a: Dependence of the edge compression ε_0 on the strength of the cube and the degree of loading κ of the bending pressure body

Table 3a: first lines: experimental values ε_0, second lines: experimental values κ, third lines: hypothetical values $\hat{\kappa}$

W=80	0.06	0.13	0.20	0.30	0.41	0.55	0.76	1.06	1.61
	.1	.2	.3	.4	.5	.6	.7	.8	.9
	.0903	.1869	.2747	.3859	.4906	.6005	.7230	.8282	.8770
W=120	0.08	0.16	0.24	0.35	0.48	0.64	0.86	1.16	1.70
	.1	.2	.3	.4	.5	.6	.7	.8	.9
	.1029	.1968	.2823	.3872	.4939	.6023	.7158	.8168	.8856
W=160	0.09	0.18	0.28	0.40	0.55	0.72	0.94	1.24	1.77
	.1	.2	.3	.4	.5	.6	.7	.8	.9
	.1021	.1956	.2900	.3909	.5000	.6028	.7076	.8074	.8920
W=225	0.11	0.22	0.33	0.47	0.64	0.82	1.05	1.35	1.83
	.1	.2	.3	.4	.5	.6	.7	.8	.9
	.1066	.2041	.2931	.3950	.5030	.6002	.7018	.8014	.8987
W=300	0.12	0.26	0.39	0.55	0.72	0.92	1.15	1.44	1.88
	.1	.2	.3	.4	.5	.6	.7	.8	.9
	.1005	.2084	.3001	.4024	.4993	.5990	.6964	.7958	.9044
W=450	0.17	0.34	0.51	0.69	0.88	1.10	1.33	1.60	1.98
	.1	.2	.3	.4	.5	.6	.7	.8	.9
	.1093	.2119	.3080	.4031	.4964	.5959	.6906	.7905	.9121
W=600	0.20	0.41	0.62	0.82	1.03	1.26	1.50	1.76	2.07
	.1	.2	.3	.4	.5	.6	.7	.8	.9
	.1036	.2085	.3095	.4022	.4959	.5945	.6930	.7947	.9095

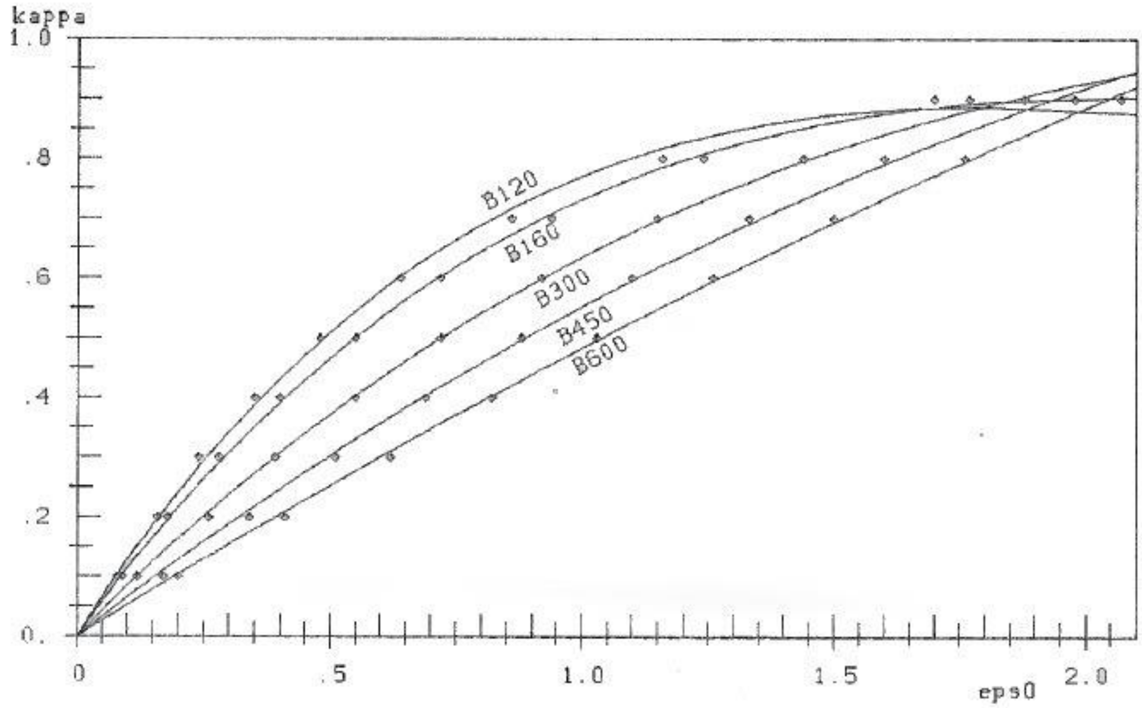

Fig. 6b: experimental points (ε, κ) and hypothetical curves (ε_0,$\hat{\kappa}$)

Table 3b: Parameters of hypothesis $\hat{\kappa}$

	a	b
W=80	1.566	.6559
120	1.345	.5579
160	1.186	.4835
225	1.012	.3951
300	.8702	.3153
450	.6634	.1842
600	.5271	.08793

In a following part III I will bring a theory of the distribution of the stress across the bending pressure zone – on the basis of these hypotheses.

Acknowledgement

I state,that this analysis could not have been done without the grand work of Rüsch and his assistants. In hard times – before 1955 . He initiated, carried through and analysed – with the then available means – an immense scientitific program, the results of which are concentrated in his 3 resulting figures 112/113/114, the basis of this work.

References

[1] Nelder J.R. and Mead R (1965). A Simplex Method for Function Minimization. The Computer Journal 7, 303-313

[2] Prentis J.M.(1951). The distribution of concrete stress in reinforced and prostrained concrete beams, when tested to destruction by a pure bending moment. University of London: City of Guilds College

[3] Rüsch H. (1955). Versuche zur Festigkeit der Biegedruckzone. Deutscher Ausschuß für Stahlbeton, Heft 120

[4] Schneeberger H. (2020). Hooke's Law: Nonlinear Generalization and Applications. Part 2: Parameters of the Bending Pressure Zone of a Beam